








ARTICLE



<https://doi.org/10.1038/s41467-020-15524-1>

OPEN

High-salt diet inhibits tumour growth in mice via regulating myeloid-derived suppressor cell differentiation

Wei He ^{1,2,3,5}, Jinzhi Xu ^{1,5}, Ruoyu Mu^{1,2}, Qiu Li ², Da-lun Lv⁴, Zhen Huang ¹, Junfeng Zhang ¹✉, Chunming Wang ²✉ & Lei Dong ¹✉

High-salt diets are associated with an elevated risk of autoimmune diseases, and immune dysregulation plays a key role in cancer development. However, the correlation between high-salt diets (HSD) and cancer development remains unclear. Here, we report that HSD increases the local concentration of sodium chloride in tumour tissue, inducing high osmotic stress that decreases both the production of cytokines required for myeloid-derived suppressor cells (MDSCs) expansion and MDSCs accumulation in the blood, spleen, and tumour. Consequently, the two major types of MDSCs change their phenotypes: monocytic-MDSCs differentiate into antitumour macrophages, and granulocytic-MDSCs adopt pro-inflammatory functions, thereby reactivating the antitumour actions of T cells. In addition, the expression of p38 mitogen-activated protein kinase-dependent nuclear factor of activated T cells 5 is enhanced in HSD-induced M-MDSC differentiation. Collectively, our study indicates that high-salt intake inhibits tumour growth in mice by activating antitumour immune surveillance through modulating the activities of MDSCs.

¹State Key Laboratory of Pharmaceutical Biotechnology, School of Life Sciences and Medical School of Nanjing University, 163 Xianlin Avenue, Nanjing 210093, China. ²State Key Laboratory of Quality Research in Chinese Medicine, Institute of Chinese Medical Sciences, University of Macau, Taipa, Macau SAR. ³Department of Immunology, School of Basic Medical Sciences, Anhui Medical University, Hefei 230032, China. ⁴Department of Burn and Plastic Surgery, First Affiliated Hospital of Wannan Medical College, Jinghu District, Wuhu City, Anhui Province 241000, China. ⁵These authors contributed equally: Wei He, Jinzhi Xu. ✉email: jfzhang@nju.edu.cn; cmwang@umac.mo; leidong@nju.edu.cn

Excessive intake of dietary salt (NaCl) is clearly defined as an unhealthy lifestyle, due to its strong correlation with higher risks of chronic inflammation¹, cardiovascular disease² and autoimmune diseases³. Therefore, many professional societies recommend an upper salt intake limit of 3.75–6 g per day⁴. Growing evidence suggests that high-salt intake causes dysfunction in innate and adaptive immune responses. For instance, a high-salt diet (HSD) has been shown to activate interleukin (IL)-17-producing helper T (Th17) cells *in vivo* and exacerbate autoimmune encephalomyelitis (EAE) and cerebrovascular diseases^{5,6}. Meanwhile, a high level of NaCl weakens the suppressive capacity of regulatory T cells on immune reactions, and promotes the secretion of many inflammatory cytokines, such as interferon (IFN)- γ ⁷. In addition, under high-salt stimulation, macrophages polarise towards a typical M1 phenotype, secreting more pro-inflammatory cytokines, reactive oxygen species (ROS) and nitric oxide synthase 2 (NOS2), and activating inflammasome-related pathways^{8–11}. These findings suggest that high-salt intake promotes inflammation in various tissue microenvironments, which may induce inflammatory diseases such as rheumatoid arthritis (RA) and colitis^{12,13}. However, in the tumour microenvironment, stimulating the pro-inflammatory activities of multiple cell types is key to overcoming the established immunosuppression and consequently restoring immune attack against the tumour.

Myeloid-derived suppressor cells (MDSCs) play essential roles in tumour-induced immune tolerance^{14,15}. MDSC expansion in lymphoid organs (the spleen, bone marrow and so on), blood, and tumours has been detected in tumour-bearing mice and cancer patients¹⁶. MDSCs are immature myeloid cells (IMCs) that are classified into two major subsets: monocytic MDSCs (M-MDSCs) and granulocytic MDSCs (PMN-MDSCs)^{17,18}. Both have strong immunosuppressive activities but distinct functional and biochemical characteristics¹⁹. Meanwhile, as myeloid-derived monocyte precursors, MDSCs are highly plastic²⁰. In response to various circumstance factors, M-MDSCs can differentiate into macrophages or dendritic cells (DCs)²¹, and both M-MDSCs and PMN-MDSCs can dramatically change from being immunosuppressive to immunostimulatory. The stimulation can be external factors, such as cytokines and extracellular membrane components, or internal signals, such as tumour growth factor (TGF)- β , sirtuin 1 and paired Ig-like receptor B^{22–24}. As a typical environmental stress sensed by cells, hypertonicity induced by high-salt intake can trigger immune responses in macrophages mediated by transcription factors, such as the tonicity-responsive enhancer-binding protein (NFAT5)²⁵. Studies have demonstrated that the p38/NFAT5 axis enhances the expression of a number of pro-inflammatory genes and the survival of macrophages^{26,27}. However, whether high-salt intake similarly influences the functions of MDSCs in the body is unknown.

Based on the above evidence, we hypothesise that HSD can inhibit tumour progression through priming MDSCs in the tumour microenvironment into an immunostimulatory phenotype. To explore this possibility, we establish two allograft tumour models in mice given a HSD and examine the effect of the HSD on tumour growth. Interestingly, our results suggest that HSD, though recognised as an unhealthy dietary pattern, dramatically regulates the differentiation of MDSCs in the tumour niche, leading to the removal of local immune suppression and inhibition of tumour progression.

Results

HSD retarded allograft tumour growth in murine models. To investigate the effect of HSD on tumour growth, we established two grafted tumour models in female wild-type C57BL/6 and BABL/c mice: a mouse melanoma model established by

implantation of B16F10 cells and a mouse mammary cancer model established by implantation of 4T1 cells. After 1 day of starvation, mice were subcutaneously injected with 4T1 or B16F10 cells. These mice were then fed a normal-salt diet (NSD) or HSD. The HSD-treated mice of both tumour models showed a lower tumour weight (Fig. 1a) and size (Fig. 1b) than the corresponding NSD-treated mice. The overall survival of the mice is shown in Fig. 1c. HSD prolonged the survival of the tumour-bearing mice, and more than 50% of mice on HSD survived for more than 5 weeks, whereas NSD mice died within 6 weeks. Figure 1d shows the tumours harvested after 16 days of the different treatments. Histologic analysis further revealed that HSD caused large necrotic areas in the tumour tissues (Supplementary Fig. 1a, b). HSD was also effective in decreasing tumour size (Fig. 1a, b) and prolonging tumour-bearing survival (Fig. 1c) in male tumour-bearing mice, indicating that the effects of HSD were not limited by gender. In addition, we also examined the food and water intake of tumour-bearing mice during the HSD period, and found that HSD markedly increased the food and water intake of mice (Supplementary Fig. 2a, b). To our surprise, the body weights of tumour-bearing mice were not affected by HSD, but were consistently lower than the weights of tumour-free mice (Supplementary Fig. 2c). Finally, we also investigated whether HSD impacted the general health of the animals and found no marked differences in spleen, liver or kidney indexes between the NSD and HSD groups (Supplementary Fig. 3a–f). Meanwhile, mice fed the HSD for 16 days did not exhibit hepatotoxicity or nephrotoxicity, demonstrated by a lack of differences in the serum levels of alanine transaminase (ALT), aspartate aminotransferase (AST), blood urea nitrogen (BUN) or creatinine (Supplementary Fig. 3g–j). Together, the data suggested that HSD inhibited the growth of transplanted tumours *in vivo*.

HSD-enhanced osmotic stress via increasing NaCl storage. To analyse the mechanism by which HSD retarded tumour growth, we first evaluated the effects of HSD on Na⁺, K⁺ and Cl[−] storage and water content within different organs of the tumour-bearing mice by atomic absorption spectroscopy or titration. Although the Na⁺ and Cl[−] contents were higher in the thymus, livers, spleens and tumours in HSD mice than in NSD mice of both grafted tumour models, with Na⁺ storage at its highest in the tumours (Fig. 2a and Supplementary Fig. 4a), no differences were observed in the serum, hearts or lungs of mice fed with NSD or HSD for 16 days (Fig. 2a, b, Supplementary Fig. 4a, b). Furthermore, there were no marked differences in K⁺ or water content within these organs and serum between the NSD and HSD groups (Supplementary Fig. 4c–e). We also examined Na⁺, K⁺ and Cl[−] storage in the tumours by X-ray fluorescence spectrometry, and found that HSD enhanced Na⁺ and Cl[−] storage but did not affect K⁺ content in the tumour tissue (Fig. 2c, Supplementary Fig. 4f). Sodium is essential for the distribution of body fluids and maintenance of osmotic stress. Therefore, we further investigated the effects of HSD on the osmotic pressure in these organs of tumour-bearing mice by vapour-pressure osmometry (Vapro Wescor 5520). In both tumour models, there were no significant differences in the osmolality of serum, hearts or lungs in mice fed with NSD or HSD for 16 days (Fig. 2d, Supplementary Fig. 4g). However, the thymus, livers, spleens and tumours were clearly hyperosmolar in mice with HSD. Remarkably, among these tissues, tumour tissues from mice with HSD had the highest hyperosmolality, consistent with the high NaCl accumulation within the tumour (Fig. 2d, Supplementary Fig. 4g), indicating that salt enhanced osmotic stress by accumulating sodium storage within tumour tissues. Together, these data

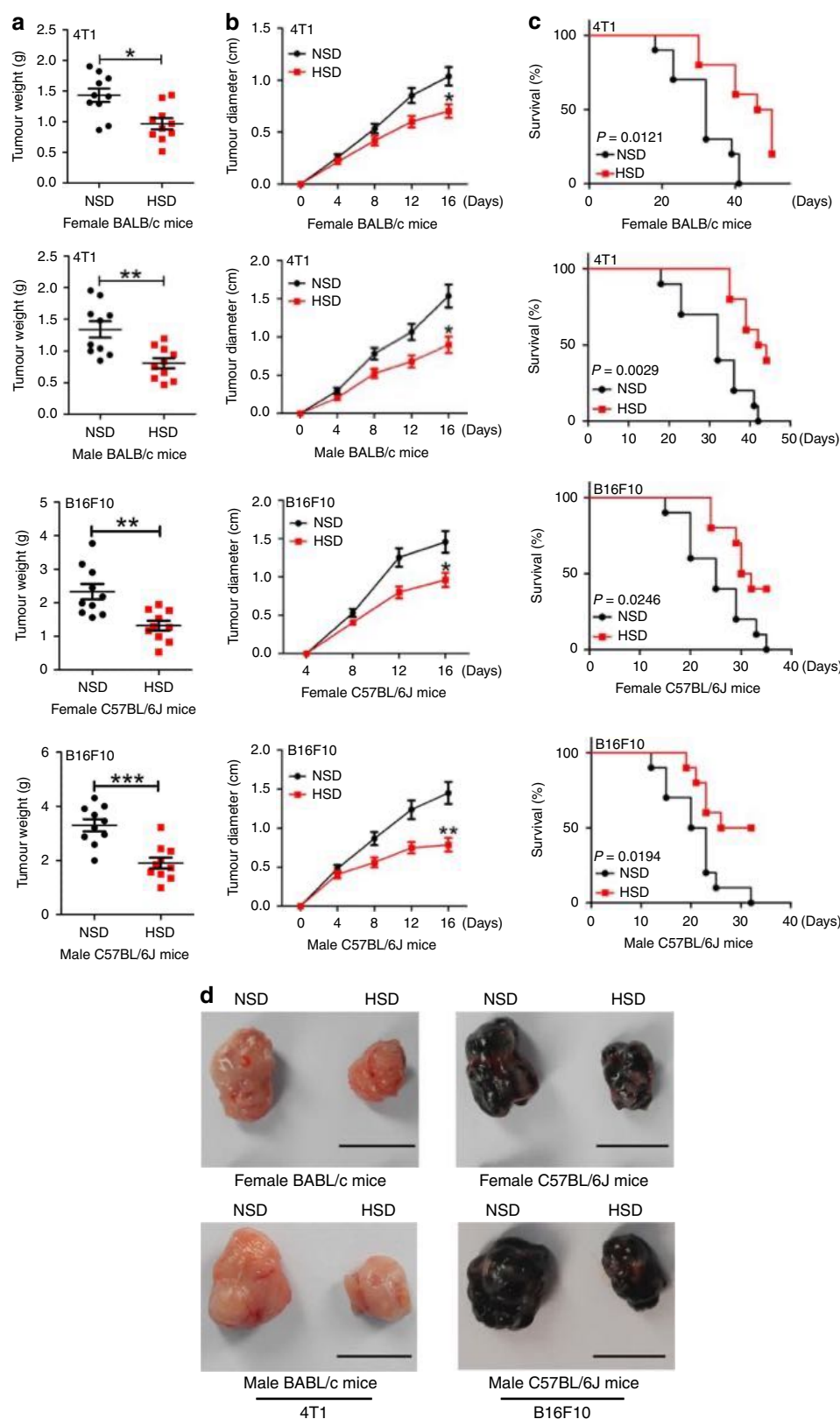


Fig. 1 HSD retarded allograft tumour growth. NSD- or HSD-fed mice were subcutaneously injected with tumour cells until the tumour tissues were harvested. **a** Tumour weight on day 16 post implantation. **b** Tumour growth curve from mice on the NSD and HSD for 16 days after tumour cells were engrafted. **c** Survival rate of tumour-bearing mice in each treatment cohort for more than 5 weeks post implantation. **d** Representative images of tumours harvested from NSD- and HSD-fed mice. Scale bar, 1 cm. For all panels, the two-tailed Wilcoxon rank-sum tests; $n = 10$ mice per group; * $p < 0.05$, ** $p < 0.01$ and *** $p < 0.001$ vs. the NSD group. These experiments were replicated with similar results. Data are representative of three independent experiments, and are presented as the mean \pm SEM. Source data are provided as a Source Data file.

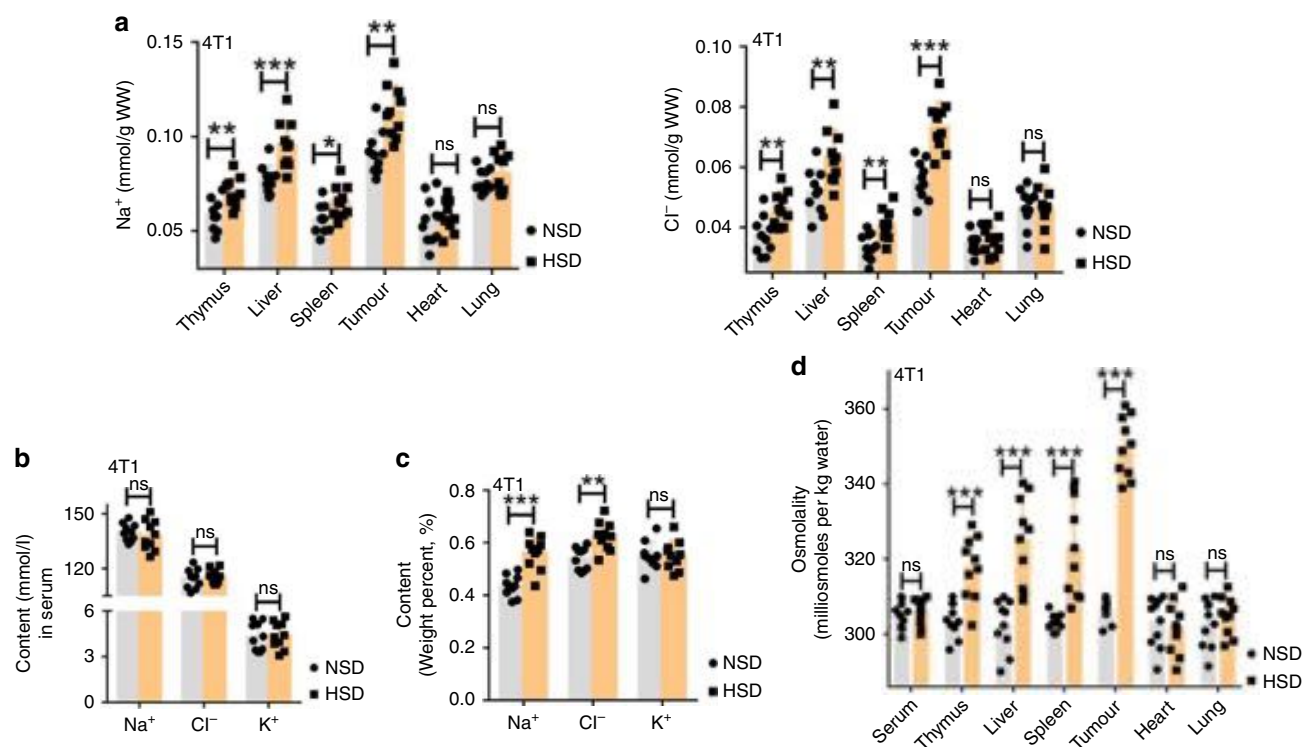


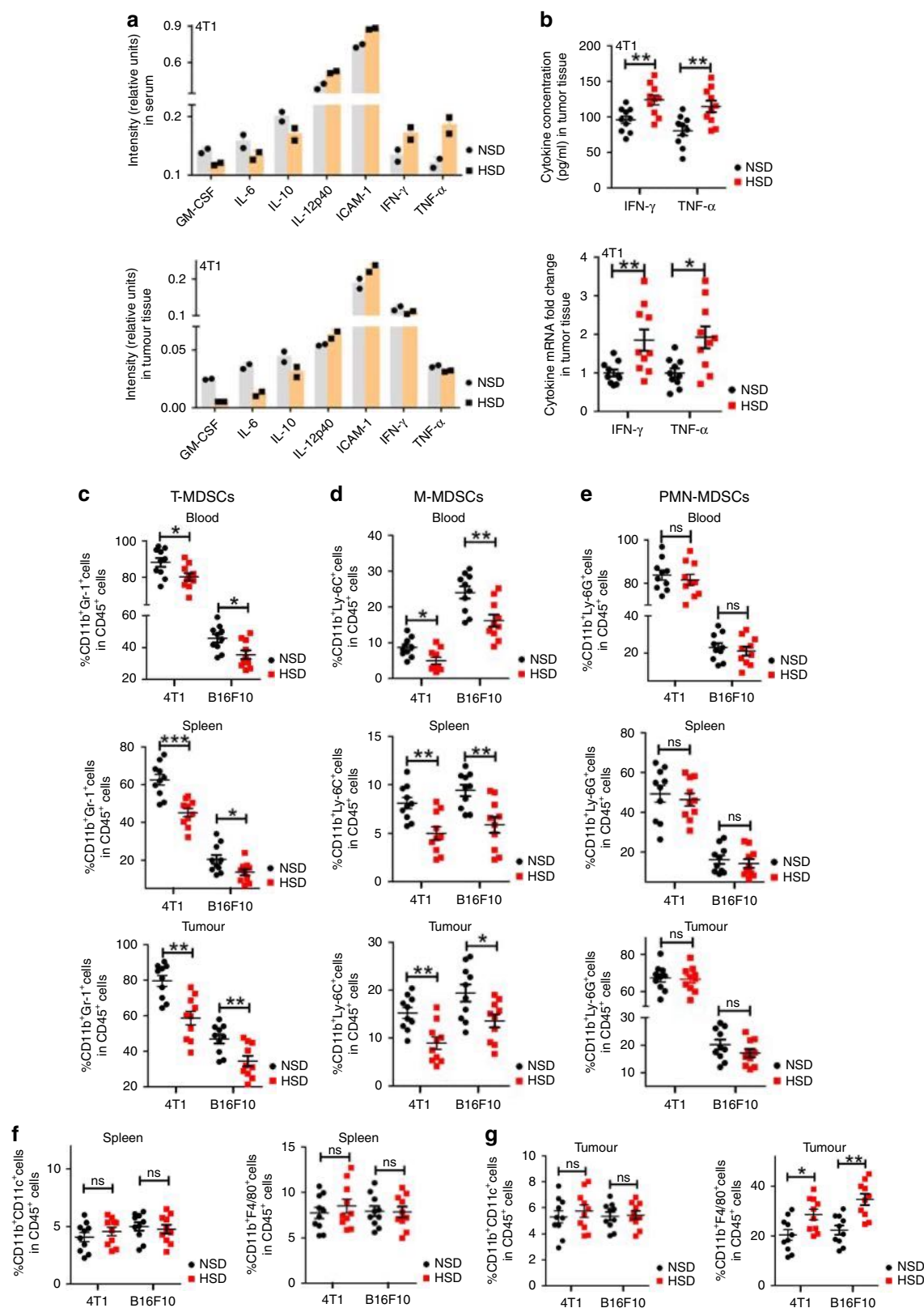
Fig. 2 HSD increased tissue osmotic stress via promoting NaCl accumulation. **a**, **b** Na^+ and Cl^- content in different organs compared with plasma concentrations in the same mice when 4T1 tumour-bearing mice were fed the NSD and HSD for 16 days. **c** Na^+ , K^+ and Cl^- content in tumour tissues was determined by X-ray fluorescence spectrometry. **d** The osmolality of tissues from 4T1 tumour-bearing mice was examined by vapour-pressure osmometry. For all panels, the two-tailed Wilcoxon rank-sum tests; $n = 10$ mice per group; ns not significant; $*p < 0.05$, $**p < 0.01$ and $***p < 0.001$. These experiments were replicated with a comparable number of mice three times. Data are representative of three independent experiments, and are presented as the mean \pm SEM. Source data are provided as a Source Data file.

demonstrated that HSD resulted in the accumulation of the salt in some mouse tissues, especially tumour tissues, causing a significant hyperosmolality in tumours. The osmotic stress likely triggers subsequent cellular reactions in tumour tissue.

HSD-induced pro-inflammatory reactions in vivo. Emerging evidence suggests that high-salt conditions can modulate the functions and differentiation of immune cells^{7,8,28}. To determine whether HSD influences the levels of the cytokines in serum and tumours, we measured cytokine levels in different tissues using a Proteome Profiler Mouse XL Cytokine Array (Ray Biothech). Compared with NSD, HSD significantly increased the production of several pro-inflammatory cytokines, including IL-12p40 and intracellular adhesion molecule (ICAM)-1, and decreased the level of IL-6, IL-10 and granulocyte-macrophage colony-stimulating factor (GM-CSF) in serum and tumour tissues from 4T1 tumour-bearing mice (Fig. 3a, Supplementary Fig. 5a). In addition, further verification of the level of IFN- γ and tumour necrosis factor (TNF)- α in tumour tissues by ELISA or qRT-PCR revealed that HSD also increased the level of IFN- γ and TNF- α in 4T1 tumours, as shown in Fig. 3b. Moreover, the results in the B16F10 tumour model (Supplementary Fig. 6a, b) were similar to those in the 4T1 model. These results suggested that the tumour growth-inhibiting effects of HSD might be due to changes in immune-system reactions.

HSD promoted MDSC differentiation in vivo. GM-CSF and IL-6 are known to inhibit myeloid precursor differentiation, inducing an increase in the number of MDSCs^{29,30}. Therefore, we investigated whether the inhibitory effects of HSD on tumour

growth were due to changes in MDSC differentiation or function. We first studied the influence of HSD on the amount of MDSCs in the blood, spleen and tumour tissues from animals 16 days after B16F10 or 4T1 tumour implantation. As demonstrated by the data (Fig. 3c, Supplementary Fig. 7a–c), within CD45^+ cells, HSD markedly decreased the number of MDSCs ($\text{CD11b}^+\text{Gr-1}^+$ cells) in the blood, spleen and, particularly, tumours. We further analysed the change in the distribution of M-MDSCs ($\text{CD11b}^+\text{Ly-6C}^+$ cells) and PMN-MDSCs ($\text{CD11b}^+\text{Ly-6G}^+$ cells), and found significantly fewer M-MDSCs in these tissues in HSD-fed mice than in NSD-fed mice of both tumour models (Fig. 3d, Supplementary Fig. 7a–c), while little difference was observed in the percentage of PMN-MDSCs (Fig. 3e, Supplementary Fig. 7a–c). The change in the number of M-MDSCs suggested a possible differentiation from MDSCs towards macrophages or DCs; therefore, we investigated the presence of macrophages and DCs in the spleens and tumours. HSD significantly increased the number of macrophages ($\text{CD11b}^+\text{F4/80}^+$ cells) in the tumour tissue, but did not alter the number of macrophages in the spleen (Fig. 3f, g, Supplementary Fig. 7b, c). Moreover, there was no significant difference in the proportion of DCs ($\text{CD11b}^+\text{CD11c}^+$ cells) within CD45^+ cells from the NSD and HSD groups in the spleens or tumour tissues (Fig. 3f, g, Supplementary Fig. 7b, c). Recent studies have suggested that HSD may inhibit the potentially pro-tumour renin-angiotensin system (RAS)^{31,32}; therefore, we performed additional experiments to investigate this possibility. HSD had significant antitumour effects under RAS inhibition using an angiotensin-converting enzyme inhibitor (captopril) (Supplementary Fig. 8a, b, d, e). Meanwhile, although both HSD and captopril decreased the level of plasma angiotensin II (AngII), the level of



plasma AngII was lower in the captopril group than in the HSD group (Supplementary Fig. 8c, f), suggesting that the anti-tumour activity of HSD may be independent of RAS inhibition. Together, our results indicated that HSD might exert its anti-tumour effects by promoting the differentiation of M-MDSCs into macrophages.

HSD-regulated MDSC differentiation and function. The above data suggested that HSD-induced hyperosmolality might have an impact on M-MDSC differentiation and function. To address this, we isolated M-MDSCs from the tumour tissues harvested from 4T1 or B16F10 tumour-bearing mice NSD- or HSD-fed mice and analysed their differentiation. As shown in Fig. 4a, b, after being

Fig. 3 The effect of HSD on inflammatory cytokine expression and MDSC differentiation in vivo. **a** Tumour homogenates and serum samples were harvested and mixed at equal quantity or equal volumes. Inflammatory cytokines in tumour tissue lysates and serum from tumour-bearing NSD- or HSD-fed mice were assessed by the Proteome Profiler Mouse XL Cytokine Array, the signal intensity of the arrays was analysed using densitometry and the relative intensity (NSD vs. HSD) of individual cytokines was analysed after normalising to the positive controls on the same membrane. Each dot represents the technical replication of one phenotype. Data are from one out of two independent experiments. **b** ELISA and qRT-PCR of TNF- α and IFN- γ in tumour tissues from NSD- and HSD-fed mice. The two-tailed Wilcoxon rank-sum tests; $n = 10$ mice per group; $*p < 0.05$ and $**p < 0.01$ vs. the NSD group. Data are from one out of three independent experiments. Data are presented as dot plots extending to minimum and maximum values in one independent experiment, and bars are presented as the mean \pm SEM of 10 individual mice. **c–g** 4T1 tumour-bearing mice were fed the NSD and HSD for 16 days, and the proportions of cells in blood, spleen and tumours were evaluated by flow cytometry. **c–e** The proportions of MDSCs in blood, spleen and tumours were evaluated by flow cytometry. **f, g** The proportion of DCs and macrophages in spleen and tumour from tumour-bearing mice are shown. The two-tailed Wilcoxon rank-sum tests; $n = 10$ mice per group; ns, not significant; $*p < 0.05$ and $**p < 0.01$ vs. the NSD group. Data are from one out of three independent experiments. Data are presented as dot plots extending to minimum and maximum values in one independent experiment, and bars are presented as the mean \pm SEM of ten individual mice. Source data are provided as a Source Data file.

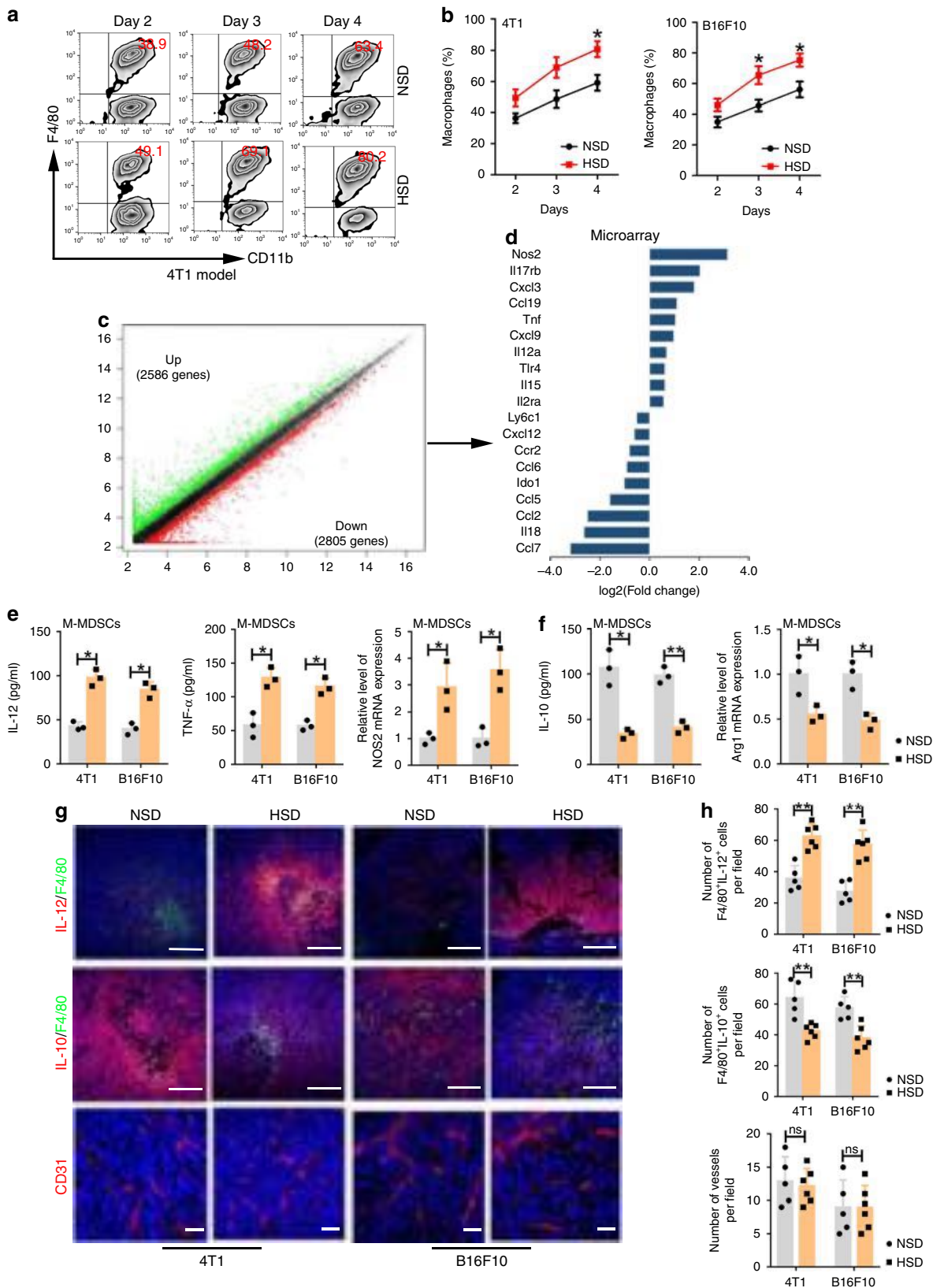
cultured for 2, 3 and 4 days, M-MDSCs from the HSD group exhibited much higher differentiation into macrophages (F4/80⁺CD11b⁺ cells) than those from the NSD group, while DC differentiation was almost the same between groups (Supplementary Fig. 9a, b). Meanwhile, the high-salt conditions used in the experiment did not influence cell viability (Supplementary Fig. 9c, d). Next, we profiled the mRNA expression of purified tumour-infiltrating M-MDSCs from the NSD or HSD group using Agilent's mouse gene chip array. As shown in Fig. 4c, we identified 5391 differentially expressed genes (DEGs) comprising 2586 upregulated and 2805 downregulated genes, with a fold change greater than 1.5 between M-MDSCs from the NSD and HSD groups. Subsequently, the results demonstrated a significant shift towards an antitumour pro-inflammatory phenotype in HSD-fed mice with a dominant increase in NOS2, TNF, IL-12a, Toll-like receptor 4 (TLR4) and chemokine (C–C motif) ligand 19 (CCL19) expression, and a decrease in lymphocyte antigen 6 complex, locus C1 (Ly6C1), C–C–C motif chemokine ligand 12 (CXCL12), indoleamine 2,3-dioxygenase 1 (IDO1) and CCL2 expression (Fig. 4d). Among these differences, the difference in the expression of IL-12, TNF- α , NOS2, IL-10 and arginase 1 (Arg1) was confirmed by ELISA or qRT-PCR (Fig. 4e, f). Furthermore, immunofluorescent staining also demonstrated significantly increased IL-12 expression and decreased IL-10 expression in the tumour tissues of HSD-fed mice. Moreover, the number of F4/80-positive macrophages in tumour tissues from the HSD group was remarkably higher than that in tumour tissues from the NSD group (Fig. 4g, h). In addition, immunofluorescence staining showed that the blood vessels in tumour tissues were not significantly affected by HSD (Fig. 4g, h). Together, these results demonstrated that HSD effectively induced M-MDSC differentiation and polarised M-MDSCs towards an antitumour and pro-inflammatory phenotype.

Although HSD did not alter the number of PMN-MDSCs in vivo, we asked whether HSD could also influence their function by switching them from a pro-tumour to an antitumour phenotype. After PMN-MDSCs were isolated from NSD and HSD tumour tissues, we investigated the effects of HSD on the immunosuppressive function of PMN-MDSCs. The T-cell proliferation assay indicated that PMN-MDSCs isolated from the HSD group lost their suppressive function and even enhanced T-cell proliferation (Supplementary Fig. 10a). We further examined the effects of HSD on ROS production, one of the main antitumour markers in PMN-MDSCs. ROS production was higher in PMN-MDSCs from the HSD group than in those from the NSD group (Supplementary Fig. 10b). Lastly, after the purified tumour-infiltrating PMN-MDSCs were cultured for 24 h in vitro, cells from the HSD group expressed more TNF- α and ICAM-1 and less prostaglandin E2 (PGE2), Arg1, CCL2 and CCL5 than those from the NSD group (Supplementary

Fig. 10c, d). These data indicated that HSD switched the function of PMN-MDSCs from an immunosuppressive state to a pro-inflammatory and antitumour one.

HSD enhanced T-cell-mediated antitumour responses. MDSC accumulation was associated with a reduction in T-cell-mediated antitumour activity during tumour progression³³. Therefore, we investigated whether promoting MDSC differentiation and inhibiting its immunosuppressive functions by HSD would affect the proliferation and functions of CD4⁺ T and CD8⁺ T cells in tumour animal models. First, we evaluated the total percentages of T cells in the blood, spleen and tumour tissues of the HSD-fed mice compared with those in NSD-fed mice. As shown in Fig. 5a–d, HSD increased the frequencies of CD4⁺ T and CD8⁺ T cells within CD45⁺ cells by ~50% in these tissues of both 4T1 and B16F10 tumour models. Consistent with these data, the proliferation status of CD4⁺ and CD8⁺ T cells within tumours was greater in HSD-treated animals than in NSD-treated animals (Fig. 5e, f, Supplementary Fig. 11a–d). We further showed that HSD treatment resulted in an augmented frequency of IFN- γ -producing CD4⁺ and CD8⁺ T cells in the spleen and tumour of treated mice (Fig. 5g–i, Supplement Fig. 12a, b), indicating a highly activated state of these intratumoural T cells. Meanwhile, HSD significantly reduced the proportion of tumour-induced Tregs in the spleens and tumours of the animal models (Fig. 5g, h, Supplementary Fig. 12c). Studies have recently demonstrated that a high-salt environment could promote the generation of pathogenic Th17 cells with upregulated TNF- α production. Therefore, we investigated whether HSD affected Th17 cell differentiation and the related cytokine expression, and found that HSD enhanced the number of Th17 cells and induced TNF- α expression in tumour tissues (Fig. 5j, Supplementary Fig. 12d). Furthermore, to further confirm the contribution of T cells to the antitumour effect of HSD, we established the two tumour models in the BABL/C-*nu/nu* mice^{34,35}. As these mice lack sufficient T-cell-mediated immune reactions, we found no differences in tumour growth indexes (tumour weight and size) between the NSD and HSD groups in the BABL/C-*nu/nu* mice (Supplementary Fig. 13a–f), further demonstrating that the T-cell-mediated antitumour response was key to the HSD-induced antitumour activity.

HSD enhanced the antitumour activation of PD-1 inhibition. MDSCs are a highly immunosuppressive population of IMCs that contribute to tumour immune escape by inhibiting antitumour T-cell activity, thereby reducing the efficiency and efficacy of immunotherapies that involve the activation of T cells^{36,37}. Therefore, we hypothesised that HSD would impair MDSC function and enhance T-cell-mediated tumouricidal effects,



improving the effectiveness of immune checkpoint therapies in cancer treatment. To prove this hypothesis, we examined the effects of HSD treatment in combination with a mouse checkpoint inhibitor, an anti-PD-1 antibody, in 4T1 and B16F10 tumour models. As shown in Fig. 6a–c, treatment with HSD or

the anti-PD-1 antibody alone resulted in a marked retardation of tumour growth across the studied models. However, the combination of HSD and the anti-PD-1 antibody achieved the highest tumour-suppressive response in both the 4T1 and B16F10 model. Furthermore, the combination of HSD and the anti-PD-1

Fig. 4 HSD promoted MDSC differentiation and functional transformation. **a, b** M-MDSCs purified in tumour tissues from the NSD or HSD group were cultured in RPMI-1640 medium containing 10% FBS and 10 ng ml⁻¹ GM-CSF for 2, 3 or 4 days. Population of CD11b⁺F4/80⁺ cells was evaluated by flow cytometry. One-way ANOVA with post hoc Bonferroni correction; $n = 10$ mice per group; $*p < 0.05$. Bars are expressed as the means \pm SEM of three replicates. **c, d** mRNA expression was examined using Agilent Mouse GE v2 Microarrays (4 \times 44 k format) after tumour-infiltrating M-MDSCs were isolated from the NSD or HSD group. DEGs in the chip analysis and mRNA expression levels of representative HSD-regulated genes involved in MDSC function from the HSD group; $n = 5$ for the NSD group and 6 mice for the HSD group. **e, f** Tumour-infiltrating M-MDSCs from the NSD or HSD group were cultured in RPMI-1640 medium containing 10% FBS for 24 h. The concentrations of IL-12, TNF- α and IL-10 in the supernatant were tested by ELISA, and NOS2 and Arg1 mRNA expression levels were examined by qRT-PCR. Two-tailed Student's t test; $n = 5$ for NSD and six mice for the HSD group; $*p < 0.05$ and $**p < 0.01$. Bars are expressed as the mean \pm SEM of three independent replicates with isolated cells pooled from the same group of mice. **g, h** The effects of HSD on macrophage infiltration, IL-12 and IL-10 levels and angiogenesis (CD31) in tumour tissues were evaluated by immunofluorescent imaging. Green, F4/80; blue, DAPI nuclear staining; red, IL-12, IL-10 or CD31; scale bar, 100 μ m. The number of F4/80⁺IL-12⁺ cells, F4/80⁺IL-10⁺ cells and vessels (CD31⁺ cells) in high-power optic (for F4/80⁺IL-12⁺ cells, F4/80⁺IL-10⁺ cells, $\times 200$ magnification; for vessels (CD31⁺ cells), $\times 400$ magnification) field in stained sections (5 fields for each section; $n = 5$ individual tumours in the NSD group and $n = 6$ individual tumours in the HSD group). The two-tailed Wilcoxon rank-sum tests; $n = 5$ for the NSD group and 6 mice for the HSD group; ns not significant; $**p < 0.01$. Bars are expressed as the mean \pm SEM. $n = 5$ data points for the NSD group and 6 data points for the HSD group (the average number of five fields for each section). For all panels, experiments were repeated twice. Source data are provided as a Source Data file.

antibody significantly increased infiltration of T cells in tumour tissues (Fig. 6d–f). The data suggested that HSD is a promising strategy to enhance the efficacy of PD-1 immune checkpoint inhibitors in cancer treatment.

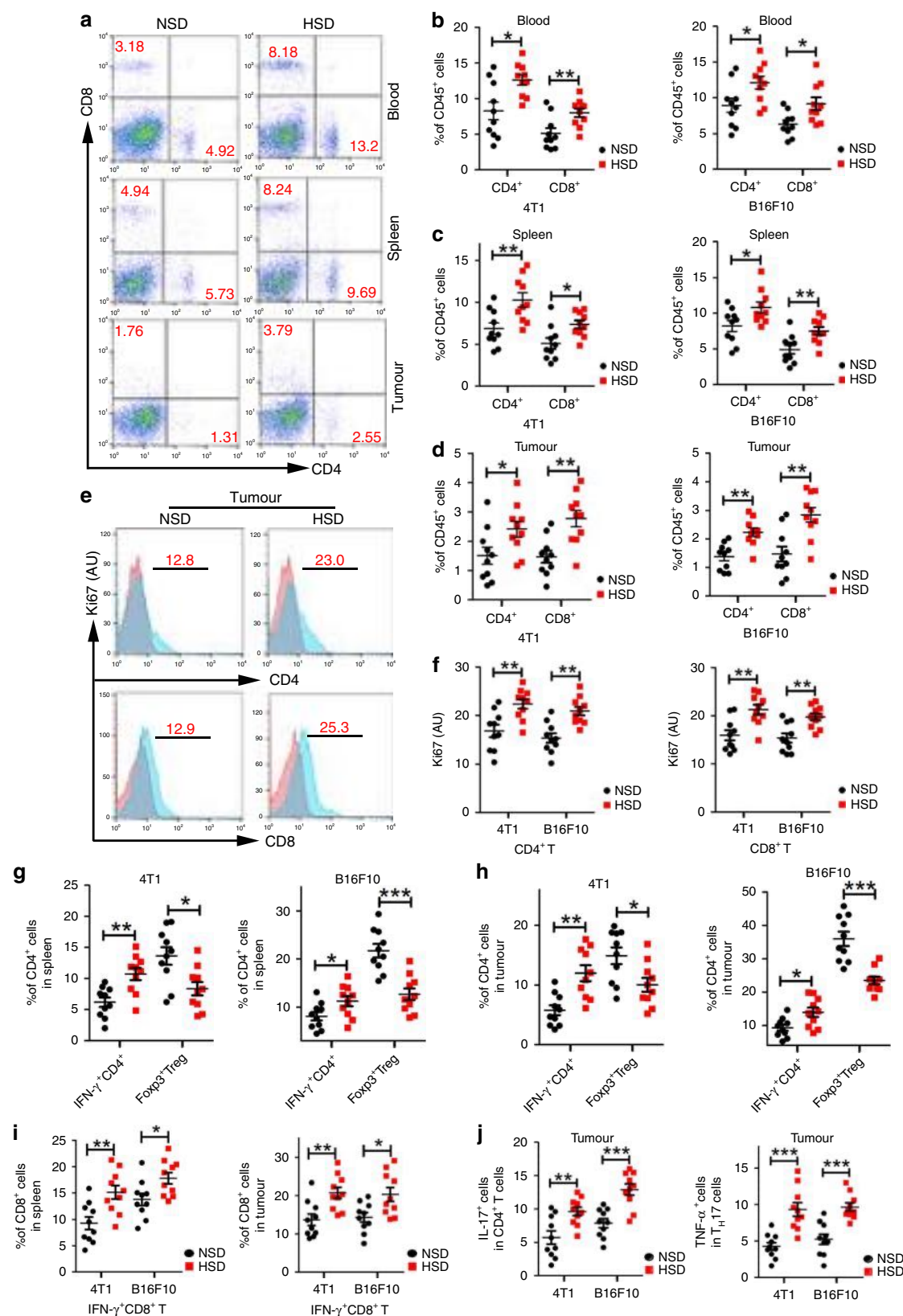
HSD-regulated p38/MAPK–NFAT5 signalling. We sought to explain the mechanism by which HSD regulates the differentiation and function of M-MDSCs. First, we analysed cellular processes enriched in DEGs in M-MDSCs isolated from tumour tissues from HSD-fed mice. Interestingly, the 2586 DEGs upregulated (fold change > 1.5) in M-MDSCs from the HSD group were markedly enriched in processes involving cytokine production, cell chemotaxis, IFN- γ production, cell maturation, osmotic stress responses and acute and inflammatory responses (Figs. 4c and 7a). The DEGs related to osmotic stress responses suggested that osmotic stress might be the predominant cellular process represented in the M-MDSCs from the HSD group. From the chip analysis, we found that HSD could also activate the c-Jun N-terminal kinase (JNK) and nuclear factor (NF)- κ B pathway (Fig. 7a), and recent studies have suggested that hypertonic stress in mammals is sensed by p38 mitogen-activated protein kinase (p38/MAPK)^{38,39}. Therefore, we investigated whether salt influences these pathways in MDSCs *in vitro* by increasing the concentration of NaCl in the media (an additional 40 mM, referred to as high-salt conditions according to previous reports^{40–42}). As shown in Fig. 7b and Supplementary Fig. 14a, b, activation in the presence of this additional 40 mM NaCl for 1 h augmented the phosphorylation of p38/MAPK, but had no effect on JNK phosphorylation or NF- κ B activation in M-MDSCs. Meanwhile, high salt promoted the differentiation of M-MDSCs into macrophages, as well as increases M1 marker (TNF- α , IL-12 and NOS2) expression and decreased M2 marker (IL-10 and Arg1) expression. Silencing of p38 blunted this effect of the high-salt conditions (Supplementary Fig. 15a–c). Surprisingly, high-salt stimulation for 24 h, upregulated JNK phosphorylation and NF- κ B activation in M-MDSCs, but p38 silencing blunted JNK phosphorylation and NF- κ B activation (Fig. 7c, d), suggesting that high salt indirectly regulated JNK and NF- κ B signalling cascades via the p38/MAPK pathway. In conclusion, HSD might boost MDSC differentiation and function via the p38/MAPK pathway.

A key transcription factor (TF) involved in the hypertonic stress-induced p38/MAPK cascade is the osmosensitive TF NFAT5^{43,44}. Analysis of the microarray dataset indicated that the expression of two key TFs (activating TF 2 [ATF2] and NFAT5) responsible for osmotic stress was enhanced in the

M-MDSCs from the HSD group (Fig. 7e). We further verified the expression of ATF2 and NFAT5 in M-MDSCs from the HSD and NSD groups in the two tumour models using qRT-PCR (Fig. 7f) and western blotting (Fig. 7g), and found that NFAT5 expression was significantly upregulated in M-MDSCs from the HSD group, but that there was no difference in ATF2 expression between the two groups in both tumour models. Lastly, we explored whether high salt (NaCl) also induced NFAT5 expression *in vitro*. Culturing in the presence of 40 mM NaCl for 24 h markedly upregulated the expression level of NFAT5 (Fig. 7h), whereas p38 deficiency reduced this response (Fig. 7i), suggesting that high-salt conditions led to a p38/MAPK-dependent NFAT5 activation.

As NFAT5 expression could be regulated by p38/MAPK, and was markedly upregulated in the high-salt conditions, we investigated whether this protein played an important role in the high-salt-mediated M-MDSC differentiation and functional transformation using an NFAT5-specific siRNA assay *in vitro*. The data shown in Fig. 8a, b suggested that there was a significant decrease in the presence of macrophages after silencing of NFAT5 under high-salt conditions. Meanwhile, the level of cytokines (TNF- α and IL-12) and the mRNA expression of NOS2 were downregulated, and IL-10 secretion and Arg1 mRNA expression were upregulated in the NFAT5 siRNA⁺ NaCl group compared with those in the control siRNA⁺ NaCl group (Fig. 8c, d). In addition, when M-MDSCs were cultured in high-salt conditions for 24 h, NFAT5 silencing reduced JNK phosphorylation and NF- κ B activation (Fig. 8e–g), indicating that NFAT5 indirectly activated the JNK and NF- κ B pathway under high-salt conditions. Importantly, western blotting revealed that NFAT5 expression was decreased by the NFAT5-specific siRNA assay (Fig. 8h).

For the *in vivo* study, we administered a lentivirus carrying NFAT5 siRNA under the Ly-6C promoter (NFAT5 siRNA-LV) or control siRNA-LV intravenously into 4T1 or B16F10 tumour-bearing mice every 2 days for 16 days. Then, we examined the expression of NFAT5 in various immune cell subsets besides M-MDSCs, such as PMN-MDSCs, macrophages and CD3⁺ T cells. As shown in Supplementary Fig. 16a–e, the lentivirus (NFAT5-siRNA-LV) could silence NFAT5 expression in M-MDSCs and macrophages, but did not affect NFAT5 in PMN-MDSCs and CD3⁺ T cells at either the mRNA or protein level. In the tumour-bearing mice treated with HSD, NFAT5 silencing in M-MDSCs and macrophages (though adoptively transferred NFAT5-deficient macrophages *in vivo* could weaken antitumour capacity²⁶) could partly restore tumour growth, because PMN-MDSC's function switch affected by HSD could also display



antitumour ability (Supplementary Fig. 17a–c). Meanwhile, the proportion of M-MDSCs and macrophages and M-MDSC functional transformation in tumour tissues was measured. Under high-salt conditions, the frequency of M-MDSCs was downregulated, and an increased proportion of macrophages in tumour tissues was observed. However, knockdown of NFAT5 in

M-MDSCs restored the proportion of M-MDSCs and inhibited the generation of macrophages in vivo (Supplementary Fig. 17d–f). Meanwhile, NFAT5 deficiency suppressed TNF- α and IL-12 secretion and NOS2 expression, and increased IL-10 and Arg1 expression under high-salt conditions (Supplementary Fig. 17g, h).

Fig. 5 HSD-enhanced antitumour immunosurveillance in vivo. **a–d** After NSD or HSD for 16 days, the frequency of CD4⁺ T cells and CD8⁺ T cells (right) and representative flow cytometry analysis (left) in the blood, spleen and tumour tissues from 4T1 tumour-bearing mice were assessed within total CD45⁺ cells. Gating strategy is provided in Supplementary Fig. 21. Data are presented as dot plots extending to minimum and maximum values in one independent experiment, and bars are presented as the mean \pm SEM of ten individual mice; the two-tailed Wilcoxon rank-sum tests; $n = 10$ mice per group; * $p < 0.05$ and ** $p < 0.01$ vs. the NSD group. **e, f** Analysis of Ki67 expression after gating on CD4⁺, CD8⁺ T cells in tumour tissues. The expression of Ki67 in CD4⁺ T cells and CD8⁺ T cells (right) and representative flow cytometry analysis (left) in the tumour tissues. Gating strategy is provided in Supplementary Fig. 21. Data are presented as dot plots extending to minimum and maximum values in one independent experiment, and bars are presented as the mean \pm SEM of ten individual mice; the two-tailed Wilcoxon rank-sum tests; $n = 10$ mice per group; ** $p < 0.01$ vs. the NSD group. **g–j** Splenic T cells and intratumoural T cells from the NSD and HSD groups were further characterised by flow cytometry. Data are presented as dot plots extending to minimum and maximum values in one independent experiment, and bars are presented as the mean \pm SEM of ten individual mice; the two-tailed Wilcoxon rank-sum tests; $n = 10$ mice per group. Two-tailed Student's *t* test; each dot represents one mouse; * $p < 0.05$, ** $p < 0.01$ and *** $p < 0.001$ vs. the NSD group. **g, h** Statistical flow cytometry plots showing the proportion of CD4⁺IFN- γ ⁺ cells and CD4⁺Foxp3⁺ Treg cells within total splenic and intratumoural CD4⁺ T cells. **i** Statistical flow cytometry plots showing the proportion of CD8⁺IFN- γ ⁺ cells within total splenic and intratumoural CD8⁺ T cells. **j** Statistical flow cytometry plots showing the proportion of Th17 cells and TNF- α ⁺ Th17 cells within tumour tissues. For all panels, these experiments were repeated twice. Source data are provided as a Source Data file.

We further evaluated whether the antitumour activity of HSD is dependent on promoting MDSC differentiation by MDSC depletion in vivo. Anti-Gr-1 antibody depleted CD11b⁺ Gr-1⁺ MDSC in tumour tissues (Supplementary Fig. 18a, b). As shown in Supplementary Fig. 18c–e, MDSC depletion using anti-Gr-1 antibodies could markedly abolish the antitumour activity of HSD, and the combination of HSD and the anti-Gr-1 antibody displayed a similar tumour growth as mice treated with NSD. The results suggested that HSD displayed the antitumour activity by regulating MDSC differentiation and function.

Finally, we isolated normal monocytes (greater than 95% purity, Supplementary Fig. 19a) from the blood of healthy mice to explore whether high-salt conditions influence monocyte differentiation via upregulating NFAT5 expression. The data indicated that high salt enhanced monocyte differentiation into macrophages. However, siRNA-mediated knockdown of NFAT5 in monocytes led to less high-salt-induced macrophage generation (Supplementary Fig. 19b–d).

These results indicated that HSD promoted the differentiation and functional transformation of M-MDSC, even normal monocytes, through p38/MAPK-dependent NFAT5 activation.

Discussion

HSDs have drawn extensive attention for their negative effects on our health, from worsening of autoimmune disease to increased risk of cardiovascular diseases, obesity, diabetes and fatty liver, with evidence from recent studies^{45–47}. On the other hand, new evidence has demonstrated that high-level salt in vivo might contribute to cutaneous antibacterial defences, suggesting that HSD could also be beneficial in skin defence⁴⁸. A recent study also suggests its implication on tumour development²⁸. In the present study, we found that HSD resulted in significant accumulation of salt in tumour tissue, modulated MDSC differentiation and function, restored immune surveillance and eventually retarded tumour growth in mouse cancer models.

The expansion of MDSCs has been widely documented in studies on cancer patients as well as in many animal tumour models³⁶. Accumulating evidence has suggested that, upon entering the tumour environment, M-MDSCs quickly differentiate into tumour-associated macrophages (TAMs), leading to enhanced IL-10 secretion and impaired T-cell response^{49,50}. Recent studies have suggested that M-MDSCs are an important source of TAMs accumulated in tumour tissue⁵¹. Therefore, interference in MDSC differentiation and subsequent functionalisation might be useful in tumour therapy. PIR-B deficiency has been shown to promote MDSC differentiation into M1 macrophages and block tumour growth²³, consistent with our present results that M-MDSCs differentiating into M1 macrophages

retarded tumour growth in HSD-fed animals. In addition, according to several studies, based on their functional phenotypes, PMN-MDSCs can be divided into the N1 subgroup, with pro-inflammatory activities, or N2 subgroup, with immunosuppressive and tumour-promoting effects^{24,52,53}. Our results indicated that PMN-MDSCs from tumour-bearing HSD-fed mice exhibited an N1 (rather than N2 in NSD-fed animals) phenotype in the tumour environment, relieving more immunosuppression in the tumour microenvironment. Interestingly, the elimination of Gr-1⁺ cells by anti-Gr-1 antibody abolished the effect of HSD on tumour growth, suggesting that MDSCs play an essential role in the antitumour activity of HSD, though anti-Gr-1 antibody may also affect IMCs, MDSCs and neutrophils (studies have shown that IMCs differentiate into MDSCs in cancer, and PMN-MDSC are pathologically activated neutrophils^{54,55}). Our data also showed that HSD inhibited *T_{reg}* generation possibly through the function of MDSC, which can be compared with other finding that increasing the NaCl concentration in vivo directly impaired Treg functions and resulted in a Th1-type effector signature⁷.

We investigated the mechanism by which HSD promoted M-MDSC differentiation towards macrophages with an antitumour phenotype. Through functional enrichment analysis, we demonstrated that the osmotic stress response was one of the major cell processes represented by the DEGs in M-MDSCs in the HSD group. This phenomenon was consistent with the accumulation of salt found in tumour tissues. Previous studies have found that the p38/MAPK pathway regulates NFAT5 in response to high salt, further mediating cellular protective effects and activation of other signalling pathways including inflammatory responses^{6,25,56}. In addition, NFAT5 has been implicated in the pathogenesis of autoimmune diseases, such as RA²⁷, autoimmune type 1 diabetes (T1D)⁵⁷ and EAE³. Upregulated expression of NFAT5 was found in the synovia of patients with RA, and NFAT5 deficiency markedly inhibited the progression of an arthritis model⁵⁸. Mechanistic studies suggested that activation of the NFAT5 signal could boost the induction of Th17 cells. Moreover, NFAT5 was likely involved in the regulation of Treg activities. In addition to regulating T cells, NFAT5 has also been suggested to significantly increase the expression of IL-12 in macrophages, strengthening the M1 phenotype of the cells²⁶, which inspired us to investigate the possibility that HSD could direct the differentiation of M-MDSCs into M1 macrophages in tumours via p38-dependent NFAT5 activation. Our data indicated that under a high-salt environment, the p38/NFAT5 axis boosted JNK phosphorylation and NF- κ B activity in vivo and in vitro, which contributes to M-MDSC differentiation towards M1 macrophages. To our knowledge, our work provides the first evidence that HSD retards tumour growth via the p38/NFAT5 axis in MDSCs.